10-15-2021

Land-use dynamics associated with mangrove deforestation for aquaculture and the subsequent abandonment of ponds

Aslan Aslan

Abdullah F. Rahman
The University of Texas Rio Grande Valley

Scott M. Robeson

Muhammad Ilman

Recommended Citation
Aslan, Aslan, Abdullah F. Rahman, Scott M. Robeson, and Muhammad Ilman. "Land-use dynamics associated with mangrove deforestation for aquaculture and the subsequent abandonment of ponds." Science of The Total Environment 791 (2021): 148320. https://doi.org/10.1016/j.scitotenv.2021.148320

Land-Use Dynamics Associated with Mangrove Deforestation for Aquaculture and the Subsequent Abandonment of Ponds

Aslan Aslan[1,2*], Abdullah F. Rahman[3], Scott M. Robeson[4], Muhammad Ilman[5]

[1]PT Hatfield Indonesia, Plaza Harmoni Unit B5-B7, Jl. Siliwangi, Bogor, Jawa Barat 16131, INDONESIA
[2]Innovation Center for Tropical Science (ICTS), Sukadamai Green Residence D2 Sukadamai, Tanah Sareal, Bogor, Jawa Barat, 16165, INDONESIA
*Corresponding author: aslan@hatfieldgroup.com

[3]Coastal Studies Lab, University of Texas Rio Grande Valley, 100 Marine Lab Drive, South Padre Island, TX 78597, USA
Email: abdullah.rahman@utrgv.edu

[4]Department of Geography, Indiana University, Bloomington, IN 47405, USA
Email: srobeson@indiana.edu

[5] Yayasan Konservasi Alam Nusantara (The Nature Conservancy in Indonesia), Graha Iskandarsyah 3rd Floor, Jl. Iskandarsyah Raya No. 66C, Kebayoran Baru, Jakarta, 12160 INDONESIA
Email: muhammad.ilman@ykan.or.id

ABSTRACT

The objective of this study was to evaluate the spatiotemporal dynamics of large area mangrove deforestation, aquaculture pond building, and the subsequent abandonment of ponds in a large delta in Indonesia, namely the Mahakam Delta. So, we developed and applied a novel methodology for exploring the lifespan of aquaculture ponds. Using historical multispectral and radar data, the lifespans of aquaculture ponds across the delta were estimated via a chronological analysis of the landscape into four different states: primary mangroves→ deforested mangroves→ ponds → abandoned/inactive ponds. Specifically, a combination of sequential classification and rule-based techniques were used to: 1) produce a time series of land cover maps from 1994 to 2015 and 2) quantify lifespans of aquaculture ponds in the delta. Results show that of the 110,000 ha of primary mangrove forests in the delta in 1994, 62% had been deforested by 2015, with a 4.5% annual rate of loss on average. The lifespan of aquaculture ponds in the delta varied between 1 and 22+ years, with most of the ponds having productive lifespans of 10 to 13 years. Ponds with relatively longer lifespans were located near the existing settlements in the delta. This study showed that the productive lifespan of most aquaculture ponds in deforested mangrove lands of Mahakam delta is relatively short, information that should be useful for developing appropriate management plans for the delta or similar coastal mangrove ecosystems. The abandoned ponds can potentially be rehabilitated for shrimp and fish production after applying appropriate restorative treatments or be targeted for mangrove restoration projects.

KEYWORDS: Mangrove deforestation, Synthetic Aperture Radar (SAR), aquaculture ponds, Indonesia.

Key Points:

- SAR data is useful for tracking dynamic changes in mangrove ecosystem.
- Time series SAR data can be used to estimate lifespan of pond.
- During 22+ years, over half of the mangrove forest in Mahakam Delta has been converted to aquaculture.

1. INTRODUCTION

Mangrove forests along tropical coastlines have been massively deforested and converted to agriculture, fisheries, and infrastructure developments. Ecologically, mangrove forests serve important functions for coastal protection, conservation of biological diversity, and protection of coral reefs and seagrass beds (Duke et al. 2007; Guannel et al. 2016; Hogarth 2015; McIvor et al. 2012). Economically, mangroves are a source of charcoal, tannin, construction materials, household equipment, medicines, fish, shrimp, crab, vegetable, and raw material for pulp and paper (Abdullah et al. 2016; Primavera et al. 2019; Rizal et al. 2018). Mangrove's unique root systems prevent erosion, capture sediment, and filter pollutants that would otherwise flow out to the ocean (Chaudhuri et al. 2019; Kathiresan and Bingham 2001). Moreover, mangrove ecosystems sequester large quantities of carbon from the atmosphere and therefore are vital to the global carbon cycle and climate change mitigation (Alongi 2020). Mangroves are well known as the most carbon-rich forests in the tropics, containing several times the amount of carbon per hectare compared to upland tropical forests (Donato et al. 2011).

Nearly one-third of the world's mangrove forests have been lost to deforestation over the past 50 years (Alongi 2002; Barbier 2014). Along with coastal development, another primary cause of global mangrove deforestation is the development of shrimp farms to support a booming fisheries export industry (Barbier and Cox 2004; Hamilton 2020; Richards and Friess 2016), with the global demand for shrimp continuing to increase (Anderson et al. 2019). A study by Hamilton (2013) revealed that 51.9% of original mangrove areas have been deforested between the 1970s and post-2004, with commercial aquaculture accounting for 28% of total mangrove loss across eight countries: Indonesia, Brazil, Bangladesh, India, Thailand, Vietnam, Ecuador, and China. These countries are dominant in mangrove holdings and global production of aquaculture shrimp. A recent FAO report has shown that the global production of cultured crustaceans for 2018 was 8.63 million tons, of which 50% of the produced volume was dominated by the shrimp species *Penaeus vannamei* (Shinn et al. 2018). In Indonesia, which contains ~26% of global mangrove forests (Hamilton and Casey 2016), nearly one million hectares or one-fourth of its original mangroves have been converted to aquaculture farms since 1800, and the peak rate of mangrove to aquaculture conversion occurred between 1970 and 2003 (Ilman et al. 2016). There is a strong indication of global mangrove conservation success as indicated by lower deforestation rates in many countries (Goldberg et al. 2020). But close attention to some areas such as Malaysia, Myanmar, and Papua are still needed as their deforestation rates are well above the global average (Friess et al. 2020).

There are currently ~250,000 ha of Indonesian aquaculture areas (or 'ponds' henceforth) that lay abandoned after they have been used for shrimp or fish production (Gusmawati et al. 2018). Pond abandonment typically is associated with and driven by various types of environmental degradation, such as soil compaction, the formation of acid sulfate soils in the bottom of ponds after a few years of active use, the advent of shrimp diseases such White Spot Disease (WSD), drop in the shrimp production due to pollution from the use of fertilizer and other chemicals, and the breach of pond gates and dykes due to a combination of high rainfall and high tide (Barbier 2012; Dierberg and Kiattisimkul 1996). In order to meet the increasing global shrimp demand, primary mangrove areas are continuously converted to ponds as others are abandoned in their degraded form. And yet, no maps currently exist showing the location of productive and abandoned shrimp ponds in any major mangrove region. Also, many mangrove areas are inaccessible or difficult to access, so effective monitoring programs are needed to document such conversion processes. Mapping spatiotemporal trends of large-scale mangrove deforestation, aquaculture ponds development, and the subsequent abandonment of ponds due to different biophysical and socio-economic reasons is the first step towards understanding the dynamics of anthropogenically modified mangrove ecosystems and developing a sustainable regime for both shrimp production and mangrove conservation.

A number of remote sensing studies using satellite and airborne multispectral images have mapped mangrove forests that vary in spatial resolutions and coverages (Aslan et al. 2016; Gao 1998; Gao et al. 2004; Giri et al. 2015; Giri et al. 2011; Giri et al. 2007; Giri et al. 2008; Green et al. 1998; Hamilton 2013; Hamilton and Casey 2016; Hansen et al. 2009; Heumann 2011; Myint et al. 2008; Rahman et al. 2013; Vo et al. 2013). Unfortunately, multispectral remote sensing using optical sensors is limited by the persistent cloud cover in the tropics, leading to inconsistent and inaccurate results. In contrast, Synthetic Aperture Radar (SAR) sensors penetrate clouds and therefore have the potential to provide consistent and systematic global datasets for accurately monitoring changes in tropical mangrove areas. Several studies have demonstrated that using SAR data in combination with optical and lidar data may result in more accurate maps of the coverage and, in some cases, structure of mangroves (Aslan et al. 2016; Bunting et al. 2018; Cougo et al. 2015; Held et al. 2003; Kovacs et al. 2013; Lagomasino et al. 2015; Lee et al. 2018; Lucas et al. 2014; Lucas et al. 2007; Nascimento Jr et al. 2013; Rocha de Souza Pereira et al. 2012; Simard et al. 2006; Trisasongko 2009).

In addition to mapping mangrove coverage and classification of mangrove species, several studies have used remote sensing data for mapping and monitoring aquaculture pond development in mangrove ecosystems (Duan et al. 2020; Dwivedi and Kandrika 2005; Gusmawati et al. 2018; Jayanthi 2011; Pattanaik and Prasad 2011; Prasad et al. 2019; Sridhar et al. 2008; Travaglia et al. 1999; Travaglia et al. 2004; Venkataratnam et al. 1997; Virdis 2013; XU et al. 2013; Zhang et al. 2010). SAR data in particular, have been used for regular monitoring surface water condition in flooded areas (Canisius et al. 2019), which in turn is very promising for aquaculture pond development mapping. Among these studies, only Gusmawati et al. (2018) mapped the abandoned ponds in Perancak, Bali, Indonesia, with accurate results and suggested that remote sensing data should be utilized in the planning process of rehabilitating the abandoned ponds. However, for mapping the abandoned ponds, they used very high-resolution commercial satellite data, which have limited areal coverage and are not economically viable for large areas (e.g., for nationwide mapping).

The objective of this study was to explore and quantify the spatiotemporal dynamics of large area mangrove deforestation, aquaculture pond development, and the subsequent abandonment of ponds. We developed and applied a suite of rule-based methods for that purpose. We used a 22-year time-series of satellite data from a severely deforested large mangrove region of Indonesia, namely the Mahakam delta, as a case study for our methodology and to investigate the land use change dynamics across the delta. A major point of emphasis was the estimation of lifespans of aquaculture ponds, which was achieved through a detailed chronological analysis of four different states of the disturbed mangrove land: 1. primary mangroves→ 2. deforested mangroves→ 3. ponds → 4. abandoned/inactive ponds. Quantifying the lifespans of aquaculture ponds is essential for developing appropriate management plans for coastal mangrove ecosystems, as the abandoned ponds can potentially be rehabilitated for shrimp and fish production after applying appropriate restorative treatments, or alternatively, the abandoned ponds can be targeted for mangrove restoration projects.

2. MATERIALS AND METHODS

2.1. Study Area

Our study area was the Mahakam Delta in the East Kalimantan Province of Indonesia. Lying between 117°15'-117°45'E and 0°15-0°45'S and covering an area of approximately

110,000 ha (Fig. 1), the land is generally flat where mangroves forests are present (in pioneer, mature, and degraded stages). Prior to 1980, the delta was almost entirely covered with mangroves (Van Zwieten et al. 2006), of which, over 50% were pure *Nypa* (Dutrieux et al., 2014). Mangroves of genus *Sonneratia* and *Avicennia* were abundant in the delta front, while genus of *Rhizophora* grew along the banks of distributaries of the lower delta. *Nypa* covered the delta's central area, and many mixed mangroves (e.g., *Avicennia*, *Sonneratia*, *Rhizophora*, *Bruguiera*, *Xylocarpus* and *Nypa*) grew in the transitional areas between the delta front and the central zone. Other mixed mangroves (e.g., *Oncosperma*, *Heritiera*, *Gruguiera* and *Excoecaria*) covered the delta's uppermost areas (Sidik 2010).

Fig. 1 goes here.

Since the late 1980s, mangroves in the Mahakam Delta have seen large-scale deforestation due to construction of ponds for growing tiger shrimp and milkfish (Bosma et al. 2012; Dutrieux et al. 2014). Mangrove deforestation in the Mahakam Delta spiked in the late 1990s, when the shrimp price increased sharply in global markets (Bourgeois et al. 2002). However, during the 2000s, due to low productivity caused by acidification of the soil, accumulation of pollutants, and lack of nutrients in the ponds, along with a drop in the shrimp price in global markets, many of these ponds were left inactive and were ultimately abandoned (Dutrieux et al. 2014; Sidik et al. 2014)

2.2. Times-Series of Satellite Data and Image Pre-processing

To generate the time-series of mangrove-to-pond conversion of the Mahakam Delta from 1994 to 2015, we used 63 images from three types of level-1 SAR data, namely the Image Precision (IMP), Single Looks Complex (IMS/SLC), and Ground Range Detected (GRD) products. All images came from four different generations of C-band sensors onboard three SAR platforms (ERS-1/2, ENVISAT, and SENTINEL-1A) and were obtained from the European Space Agency's (ESA) Client for Earth Observation Catalogue and Ordering Services (EOLi-SA server: https://earth.esa.int/web/guest/eoli). The number of SAR images covering our study area for each year varied depending on their availability in the EOLi-SA archive. The complete list of available SAR datasets used in this study and their acquisition dates are presented in Table 1.

Table 1 goes here.

These 63 SAR scenes were processed, calibrated, filtered, resampled to 30 m spatial resolution, geo-rectified to the Universal Transverse Mercator (UTM) projection (zone 50S, WGS-84 datum), and the digital number (DN) values were converted to radar backscatter values (σ^o, unit of decibels, dB) using the Next ESA SAR Toolbox (NEST) software (version 5.1). The SAR data processing steps are shown in the complete data processing flowchart for this study, presented in Fig. 2.

Fig. 2 goes here.

Because the number of SAR scenes varied from year to year, and the focus of this study was to produce yearly land cover maps, we had to perform some intermediate processing steps in order to create a composite SAR image for each year. First, we applied the minimum value composite (MinVC) technique to create a single layer derived from the available SAR images for a particular year. The MinVC technique is analogous to the maximum value composite (MVC) method introduced by Holben (1986). The rationale of using MinVC in this study, and not the MVC, was: SAR images vary in their backscatter values (σ^o) due to differences in acquisition times and seasons, but all SAR images share similar characteristics in relative σ^o reflected from certain ground surfaces. For example, waterbodies, such as ponds, tend to have the lowest σ^o compared to other terrestrial surface objects depicted in a SAR image (e.g., vegetation and bare land) because most of the incident radar pulses are reflected specularly by water in ponds. The use of MinVC technique was thus appropriate because one of our principal goals was to identify ponds. We produced 15 MinVC SAR image outputs representing 1994, 1996-2001, 2003, 2004, 2006-2010, and 2015 (data years). The years 1995, 2002, 2005, and 2011-2014 are years when no SAR data were available from the EOLi-SA archive.

In order to normalize the wide ranges of σ^o present in the MinVC images from different years, we used the first year's MinVC as the reference image (i.e., 1994) and used a radiometric normalization technique (histogram matching) to rescale the other 14 MinVC images. An additional geo-rectification adjustment was applied to each histogram-matched MinVC SAR images using a relatively cloud-free mosaiced Landsat-8 image (Path/Row 116/60 and 116/61, May 1st, 2015) as the reference image. Landsat-8 images have a small geolocation uncertainty, i.e., less than 12 m circular error (Irons et al. 2012). The spatial precision obtained for these MinVC SAR images after adjustment with the Landsat-8 image was smaller than one 30-m pixel.

In addition to the SAR images, we acquired multispectral images with the lowest cloud cover available from Landsat 5 TM, Landsat 7 ETM+, and Landsat 8 OLI satellites for the data years (even these best-available Landsat images had 20-50% cloud cover). These images were downloaded from the U.S. Geological Survey Earth Explorer data portal (http://earthexplorer.usgs.gov/) and geocoded in the UTM projection system, zone 50S and WGS84 datum. Reflectance transformations of these Landsat images were not available when we downloaded them, so we used the atmospheric correction tool (ATCOR) in ERDAS

Imagine® software to convert the Landsat DN values into surface reflectance. These reflectance images were used in selecting training areas for land-cover classification of the SAR images, as described below.

2.3. Classification Strategy for Time Series of Land Cover Maps

2.3.1. Phase-1 classification

The DN value of a SAR image pixel represents an estimate of the backscatter of objects on the ground. As a rule of thumb, higher backscatter indicates rougher targets and lower backscatter indicates smoother targets (Li and Chen 2005). As a result, it is possible to distinguish primary mangrove forests, deforested mangroves, and aquaculture ponds by the different backscatter of each target class (because they have different surface roughnesses). In this study, using the histrogram of MinVC SAR images, the presence of water within the ponds is distinguishable by the histogram very low σ^o and thus a darker shade (Fig. 3). In contrast, deforested mangroves have very high σ^o and appeared brighter on the SAR images (Fig. 3). Deforested mangroves produce high backscatter because the stubs and the large debris left after mangrove deforestation induce corner-reflector or double-bounce effect, first from bare soil (horizontal) towards vertical stubs of deforested mangrove tree and then reflected from these vertical stubs back to the sensor (Proisy et al. 2000; Wang and Imhoff 1993). Primary mangroves, on the other hand, usually have medium roughness, and they appear as moderately bright features in the SAR image as illlustrated in Fig. 3.

Fig. 3 goes here.

To identify training areas of aquaculture ponds and deforested areas, we used an RGB false color combination of SWIR, NIR, and Red reflectance bands of a Landsat image for each year. Landsat images were used as reference to SAR images to identify training areas because the spectral reflectance profiles of water, soil, and vegetation derived from multispectral imagery is well established (Jensen 2005). In this study, we considered that the mangrove areas in the Landsat imagery would have the spectral profile of vegetation, the deforested areas would have a similar spectral profile to soil, and the aqualture ponds would have the spectral profile of water. After locating these training areas, the σ^o of ponds and deforested areas in the MinVC SAR image were used as training samples to classify the entire delta using the Flexible Statistical Expert Based method (or FSEB, Aslan et al. 2016).

Table 2 goes here.

The FSEB method develops a statistical threshold for σ^o for each land cover class (such as pond) and identifies all pixels as being in that class. This method has been shown to provide a superior classification of mangrove-covered, deforested, and pond areas by minimizing the number of unclassified pixels (Aslan et al. 2016). The method is sequential and we classified the ponds first, followed by the deforested areas. After the ponds and deforested areas were classified, the remaining pixels were assigned to the primary forest class. The thresholds of σ^o for distinguishing aquaculture ponds vs. primary mangroves, as well as deforested mangroves vs. primary mangroves, varied among the individual MinVC SAR images, as shown in Table 2. These differences in σ^o threshold value may attributable to near range effect and weather condition as the fact that there is occasionally an increase in backscatter because of wind-induced roughness which can trigger waves on the ponds surface (Canisius et al. 2019). This first level of classification for mapping land cover is termed as 'phase-1' classification in this study. The procedure of identification of training pixels with Landsat images and classification of the MinVC images was repeated for all 15 years of the

SAR images. Outputs of the phase-1 land cover maps were then used in the phase-2 classification for generating a time-series of final land cover maps, as described next.

2.3.2. Phase-2 classification

After the phase-1 classification, we further categorized the deforestation class in each year's image into two sub-categories: new deforestation and past deforestation. In each year when the phase-1 classification identified an area as deforested for the very first time, that area was assigned a new deforestation class in phase-2 classification for that year. In the next available year's classification, that same area was termed as past deforestation. This differentiation was necessary because in typical mangrove deforestation, if a deforested area is not converted to aquaculture ponds for a long period of time, or if a pond is left abandoned for a long period of time, regrowth of mangroves or other coastal vegetation may occur and the σ^o in SAR images of these once-deforested land may gradually look like those of forested areas, thus introducing confusion between the estimates of primary forests and once-deforested areas.

In order to differentiate between primary forest and secondary vegetation regrowth, we analyzed the land cover maps produced in phase-1 classification using a rule-based method. The rule was: if an area was once identified as deforested, then that area would continue to be classified as 'past deforestation' in the subsequent years, even if that area's SAR σ^o were classified as 'forest' in any of those subsequent years. The only exception was: if that area became classified as aquaculture pond in a subsequent year, the classification of that area was then changed accordingly. We also used a rule-based method for the aquaculture pond class: if in a given year an area was classified as aquaculture pond for the first time in the phase-1 classification, and then in a later year it was classified as anything other than aquaculture pond, we assigned a 'non-pond' class to that area for that specific later year in the phase-2 classification. If that same area was again classified as an aquaculture pond in a subsequent year, then it was again assigned to aquaculture pond for that specific year. This practice was needed to calculate the lifespan of an aquaculture pond, as described in the next section. After completion of both phase-1 and phase-2 classifications, we produced 15 maps of land cover of the Mahakam Delta across the 22 years of our study period.

2.4. Modeling the Lifespan of Aquaculture Pond

To estimate the lifespan of aquaculture ponds, i.e., the number of years a pond was active until it became abandoned, we first extracted pixels belonging to the pond class from each of the 15 time-series of land cover maps produced in phase-2 classification. Then we used another suite of rule-based methods, as follows. The very first year when a pixel was classified as aquaculture pond was marked as the beginning, and the very last year it was still classified as aquaculture pond was marked as the ending. The range of years from the beginning to the ending was identified as the lifespan of aquaculture pond pixel. Any pixel that was classified as pond in 1994 and remained pond till 2015 was assigned a value of 22+ years, since we did not know when the 1994 pond pixels became aquaculture pond (could have been converted to pond before 1994). If a pixel was classified as aquaculture pond for a few years, then non-pond for a few years and then again aquaculture pond for a few more years, we considered the very beginning and the very ending 'aquaculture pond' years to count the lifespan of that aquaculture pond pixel. This means we considered the interim non-pond years as the time when the pond remained inactive but was not abandoned. Also, the 'gap' years of our study were not included in the calculation of beginning or ending of aquaculture pond pixel. For example, if a pixel we classified as deforested in 1994 and as aquaculture pond in 1996 (no data available for 1995 – a gap year), we considered that the pixel became aquaculture pond in 1996. In reality, that pixel could have been converted to aquaculture pond in 1995, but as we did not have the data from 1995, we did not count that gap year in estimating the lifespan of aquaculture pond pixel. A study by Sidik et al. (2014) has pointed out that 1.8 ha is the minimum size of ponds in the Mahakam Delta. As a result, we removed areas that were classified as ponds but were less than 1.8 ha in size. This decision also eliminated the problem associated with misclassification where a small area was classified as aquaculture pond, but it was in fact a part of a water-logged dike separating two adjacent ponds.

2.5. Accuracy Assessment

To examine the accuracy of our methodology in producing time series of land cover maps, we used field data from 210 ground validation points and land cover information from 163 randomly created validation points based on Google Earth (GE) images. Ground truth data were collected during 2013 and the GE images were acquired from 2014 and 2015, so we used our 2015 MinVC SAR land cover map product for the accuracy assessment. The 210 ground validation points were clustered in 14 different areas across the delta (Fig. 1) and were available from a study by Arifanti et al. (2019). That study was designed to count potential CO_2 emissions arising from mangrove conversion to aquaculture ponds, so the survey data only identifies abandoned ponds and primary mangroves. To evaluate the accuracy of our approach for active ponds and deforested lands, the 163 randomly selected GE validation points were used. Additionally, because the spatial distribution of field validation points was somewhat clustered (Fig. 1), we used the GE images to add coverage across the entire delta for the validation procedure.

The random points were selected as follows. Using the Geospatial Modelling Environment (GME) software (Beyer 2014), we randomly assigned 1,000 validation points to fall at least 100 m apart from each other over the rectangular area covering the delta, as shown in the right-hand side of Fig. 1. After removing the points that fell on the sea, mainland, rivers, channels, cloud covered areas, or the delta areas where the ground was not clearly visible in the Landsat image due to haze, a total of 163 validation points remained. Of the 163 validation points, 83 fell on ponds, 40 on primary forest, 24 on deforested mangroves, and 16 on abandoned ponds. The Kappa coefficient was used to evaluate the accuracy of 2015 land cover map classification and is presented in the form of an error matrix, which is a simple cross-tabulation of the mapped class label against the observed class in the validation data (Congalton and Green 2008).

3. RESULTS AND DISCUSSION

3.1. Mangrove Land Change Classification

The chronological sequence of the four phases of change from primary mangroves (green) → deforested mangroves (yellow) → ponds (blue) →abandoned ponds (red) caused by anthropogenic disturbance in the Mahakam Delta is strikingly apparent in our 22-year SAR time series (Figure. 4). Results from the accuracy assessment of the 2015 land cover map show a high overall accuracy of 88.7% (Foody 2002), with a Kappa statistic of 0.82. Also, the sequential classification and the rule-based approaches showed their effectiveness in classifying SAR images as illustrated by the producer's and user's (reliability) accuracy of cover types (Table 3). Given that the same C-band radar sensors obtained from EOLi-SA server and the same classification methodology were employed for all years of our study, we consider the accuracy of the land cover map classification for all other years to be similar to that of 2015.

Table 3 goes here.

Fig. 4 goes here.

3.2. Spatiotemporal Patterns of Mangrove Deforestation

In 1994, 95.7% of the study area was classified as mangrove forest (i.e., 96,300 of the 100,630-ha totals; Fig. 5). These forests constituted a single, largely contiguous tract of primary mangroves that were only separated by small channels (Fig. 4, 1994 map). Another 2.2% of the area was classified as deforested mangroves and the rest (2.1%) was classified as ponds. By 2015, the size of primary mangrove forests was reduced drastically to 37% of the study area (36,820 ha). Mangrove deforestation kept rising from 1994, with the massive change of 30,271 ha occurred in between the periods of 1997 and 2000 (Fig. 5, 'total deforestation'). The trend of increased deforestation between 1997 and 2000, as shown by our analysis, is in line with the results reported by Sidik (2010), who suggested that the peak of mangrove deforestation in the Mahakam Delta occurred between 1996 and 2000. Sidik (2010) further pointed out that, as of 2007, the loss of mangrove forest in the delta was 58,041 ha. Our findings are in support of that estimate, showing 58,790 ha of mangroves in the delta was deforested between 1994 and 2007. It is also evident that the deforestation rate decreased from 2000 to 2006 and no new deforestation occurred between 2006 and 2015 (Fig. 5). Our results indicate that the proportion of the deforested mangrove lands relative to total area of the delta was minor in 1994 (i.e., 2.2%), but drastically increased to 34.36% in 2000 and then showed a declining trend afterwards, standing at 11.7% in 2015 (Fig. 5). These findings agree with the results reported by Rahman et al. (2013), which pointed out that following 2002 the rate of deforestation in the Mahakam Delta declined every year and virtually stopped by 2009. Fig.5 also illustrates that although 'abandoned pond' was already showing an increasing trend since 1996, but significant rapid increment occurred in 2006 and afterward which may indicate declining in shrimp/fish production from aquaculture ponds in the delta.

Fig. 5 goes here.

3.3. Pond Development Patterns

As illustrated in Fig. 5, our results also indicate that there was a time lag between mangrove deforestation and pond development. In 1994, for instance, the coverage of ponds and total deforested mangroves were 2.1% and 2.2%, respectively. Yet in 2000, the area of deforested mangrove had increased to 34.4% while the area of aquaculture ponds coverage showed a relatively small increment to 7.7%. The time lag between deforestation and pond construction occurred because shrimp and fish farmers establish aquaculture ponds by manually chopping the mangroves, digging canal/trenches, and building ponds. The process could take 1-3 years, depending on the financial support available to the farmers. Results of our study revealed that ponds covered 13.5% of the Mahakam Delta in 2001, the coverage increasing rapidly to reach its peak in 2006, covering 46.2% of the delta (Fig. 5 and Table 4). The spatial extent of aquaculture ponds showed a rapid decrease from 2006 to 2010 because many of the ponds were overgrown by mangrove regeneration, although still active, or abandoned due to low productivity (Fig. 4, 5, and Table 4).

Table 4 goes here.

Our estimates on the total area of aquaculture ponds in the Mahakam Delta differ from some previously published studies. A study by Van Zwieten et al. (2006) had reported that until 2001, 75% of the delta was covered with aquaculture ponds, whereas our results indicated that during the same time period the ponds covered only about 13.5% of the delta. Another study by Dutrieux et al. (2014) pointed out that the total coverage of aquaculture ponds in 2010 was 63,000 ha, while our findings showed it to be 24,320 ha in that same year.

The discrepancies between our results and Van Zwieten et al. (2006) can be explained by the fact that they counted all deforested mangroves areas in that year as aquaculture ponds when interpreting their satellite data. In fact, it was clearly shown from the output of our two-phase classification results that there was a time lag between mangrove deforestation and aquaculture pond construction. In the case of 2010 discrepancies with Dutrieux et al. (2014), different satellite data sources and the methods of imagery interpretation used in their study resulted in differences in the extent estimation of aquaculture ponds. For instance, while Dutriex et al. (2014) used a visual interpretation method through digitizing of SAR data for classifying aquaculture ponds, we used a combination of a sequential classification and rule-based techniques. As a result, both active and abandoned ponds have been counted as ponds in Dutrieux et al. (2014), while our approach was able to differentiate betwen active and abandoned aquaculture ponds.

3.4. Lifespan of Ponds

When evaluating whether to rehabilitate ponds after a fallow period or to use the land for another purpose such as a mangrove restoration, the lifespan and age of aquaculture ponds can provide an important piece of information for sustainable mangrove management. This study demonstrated that the lifespan of aquaculture ponds in the delta ranged from 1 to 22+ years, with approximately ¾ of ponds having a lifespan that was less than 13 years (Fig. 6). While aquaculture ponds in the Mahakam Delta have been reported to reach up to 25 years of active life (Setiawan and Pertiwi 2014), other research has shown the average lifespan of aquaculture ponds throughout Asia to be 5 to 10 years due to the attendant problems of self-pollution and disease (Dierberg and Kiattisimkul 1996; Hariati et al. 1995). Likewise, other studies have pointed out that the lifespan of intensive shrimp farming does not exceed ten years (Boyd and Jason 1998). Our findings show with greater precision that the lifespan of aquaculture ponds is much more variable than previously known. This finding is significant for relevant stakeholders in aquaculture industries, especially due to the problems in acquiring new lands for establishing aquaculture farms.

Fig. 6 goes here.

The lifespan of aquaculture ponds is highly influenced by pond productivity and proximity to settlements. If a decline in productivity occurs and the locations of the ponds are in remote areas far from villages or settlements, they are more likely to be abandoned (Sidik et al. 2014). Although the ponds located near villages or settlements also decrease in production after a few years, the proximity of the villages or settlements would allow for maintenance and operational costs of the ponds to be much lower compared to those for the ponds that are in remote areas. Consequently, farmers would generally continue to cultivate shrimp/fish in the ponds near their villages despite lower yields. As a result, the lifespan of ponds near the villages and settlements tends to be longer. Our results showed that there is a propensity of the longer lifespan ponds being located near the existing villages and settlements in the delta, providing further evidence of the proximity argument as a cause of longevity of aquaculture ponds (Fig. 7).

Fig. 7 goes here.

4. CONCLUSIONS

In the coastal areas of the tropics and subtropics, mangroves ecosystems have been deforested and drastically degraded for shrimp and fish production via aquaculture. Mangrove deforestation continues in many parts of the tropics as the global demand for shrimp continues to increase. Understanding the process and precise chronology of mangrove deforestation, construction of shrimp and fish ponds, and the lifecycles of these areas is essential for developing best management practices. In this study, we presented a novel methodology for monitoring the land use dynamics of coastal mangrove areas. Using a combination of high-resolution SAR and Landsat images of the Mahakam Delta of Indonesia, along with a suite of rule-based methods of classification, we tracked the chronological sequence of four different states of mangrove land change from primary mangroves→ deforested mangroves→ ponds→ abandoned ponds from 1994 to 2015. Results of our study demonstrated that out of the 96,298 ha of mangrove forests in the Mahakam Delta, ~62% have been deforested during the study period, primarily for building shrimp and fish ponds. Pond construction rates varied over time, likely triggered by market demands, the physical condition of the ponds, and proximity to villages. This study also showed, for the first time, that the average productive lifespan of majority of the ponds in the delta is 10-13 years, with ponds having longer lifespans typically found adjacent to villages. In 2015, the total area of abandoned ponds in the Mahakam Delta was 25,744 ha or 25.6% of the study area. Currently, there is no country-level map of the many abandoned ponds that are distributed across hundreds of Indonesian islands and other major mangrove countries. Our study provides a comprehensive method that can be used to map abandoned aquaculture ponds along all the mangrove coastlines of Indonesia and other countries as well. Understanding the land use change dynamics of mangrove forests is important for all stakeholders and for sustainable management of coastal resources across the globe.

5. ACKNOWLEDGEMENTS

The authors wish to acknowledge the European Space Agency (ESA) for allowing access to SAR data used in this study via Category-1 Proposal 18389 (C1F.18389). Partial support came from NASA grant # NNX11AF50G to A.F.R. We express our gratefulness to

Ms. Virni B. Arifanti of Oregon State University, USA, and Indonesian Ministry of Environment and Forestry, for providing us with the field data for validating land cover classification.

REFERENCES

Abdullah, A.N.M., Stacey, N., Garnett, S.T., & Myers, B. (2016). Economic dependence on mangrove forest resources for livelihoods in the Sundarbans, Bangladesh. *Forest Policy and Economics, 64*, 15-24

Alongi, D.M. (2020). Global significance of mangrove blue carbon in climate change mitigation. *Sci*, 2, 67

Alongi, D.M. (2002). Present state and future of the world's mangrove forests. *Environmental Conservation, 29*, 331-349

Anderson, J.L., Asche, F., & Garlock, T. (2019). Economics of aquaculture policy and regulation. *Annual Review of Resource Economics*, 11, 101-123

Arifanti, V.B., Kauffman, J.B., Hadriyanto, D., Murdiyarso, D., & Diana, R. (2019). Carbon dynamics and land use carbon footprints in mangrove-converted aquaculture: The case of the Mahakam Delta, Indonesia. *Forest Ecology and Management, 432*, 17-29

Aslan, A., Rahman, A.F., Warren, M.W., & Robeson, S.M. (2016). Mapping spatial distribution and biomass of coastal wetland vegetation in Indonesian Papua by combining active and passive remotely sensed data. *Remote Sensing of Environment, 183*, 65-81

Barbier, E.B. (2012). Progress and challenges in valuing coastal and marine ecosystem services. *Review of Environmental Economics and Policy, 6*, 1-19

Barbier, E.B. (2014). Economics: Account for depreciation of natural capital. *Nature News, 515*, 32

Barbier, E.B., & Cox, M. (2004). An economic analysis of shrimp farm expansion and mangrove conversion in Thailand. *Land Economics, 80*, 389-407

Beyer, H. (2014). Geospatial modelling environment (GME)(Version GME 0.7. 2.1). *Melbourne, Vic.: Spatial Ecology LLC.[Google Scholar]*

Bosma, R., Sidik, A.S., van Zwieten, P., Aditya, A., & Visser, L. (2012). Challenges of a transition to a sustainably managed shrimp culture agro-ecosystem in the Mahakam delta, East Kalimantan, Indonesia. *Wetlands Ecology and Management, 20*, 89-99

Bourgeois, R., Gouyon, A., Jésus, F., Levang, P., Langeraar, W., Rahmadani, F., Sudiono, E., & Sulistani, B. (2002). Socioeconomic and institutional analysis of Mahakam delta stakeholders. *Unpublished report to Total Fina Elf, Jakarta, Indonesia*

Boyd, C.E., & Jason, W. (1998). Clay." Shrimp Aquaculture and the Environment: An Adviser to Shrimp Producers and an Environmentalist Present a Prescription for Raising Shrimp Responsibly.". *Scientific American, 278*, 58-65

Brinkman, R., & Singh, V. (1981). Rapid reclamation of brackish-water fishponds in acid sulfate soils. In, *Proc. Bangkok Symp. Acid Sulphate soils. H. Dost and N. van Breemen eds., Publ. 31, ILRI, Wageningen, 1981* (pp. 318-330)

Bunting, P., Rosenqvist, A., Lucas, R.M., Rebelo, L.-M., Hilarides, L., Thomas, N., Hardy, A., Itoh, T., Shimada, M., & Finlayson, C.M. (2018). The global mangrove watch—a new 2010 global baseline of mangrove extent. *Remote Sensing, 10*, 1669

Canisius, F., Brisco, B., Murnaghan, K., Van Der Kooij, M., & Keizer, E. (2019). SAR backscatter and InSAR coherence for monitoring wetland extent, flood pulse and vegetation: A study of the Amazon lowland. *Remote Sensing*, 11, 720

Chaudhuri, P., Chaudhuri, S., & Ghosh, R. (2019). The Role of Mangroves in Coastal and Estuarine Sedimentary Accretion in Southeast Asia. *Sedimentation Engineering*: IntechOpen

Congalton, R.G., & Green, K. (2008). *Assessing the accuracy of remotely sensed data: principles and practices*. CRC press

Cougo, M.F., Souza-Filho, P.W., Silva, A.Q., Fernandes, M.E., Santos, J.R.d., Abreu, M.R., Nascimento, W.R., & Simard, M. (2015). Radarsat-2 backscattering for the modeling of biophysical parameters of regenerating mangrove forests. *Remote Sensing, 7*, 17097-17112

Dierberg, F.E., & Kiattisimkul, W. (1996). Issues, impacts, and implications of shrimp aquaculture in Thailand. *Environmental Management, 20*, 649-666

Donato, D.C., Kauffman, J.B., Murdiyarso, D., Kurnianto, S., Stidham, M., & Kanninen, M. (2011). Mangroves among the most carbon-rich forests in the tropics. *Nature Geoscience, 4*, 293-297

Duan, Y., Li, X., Zhang, L., Chen, D., & Ji, H. (2020). Mapping national-scale aquaculture ponds based on the Google Earth Engine in the Chinese coastal zone. *Aquaculture, 520*, 734666

Duke, N.C., Meynecke, J.-O., Dittmann, S., Ellison, A.M., Anger, K., Berger, U., Cannicci, S., Diele, K., Ewel, K.C., & Field, C.D. (2007). A world without mangroves? *Science, 317*, 41-42

Dutrieux, E., Proisy, C., Fromard, F., Walcker, R., Ilman, M., Pawlowski, F., Ferdiansyah, H., & Ponthieux, O. (2014). Mangrove restoration in the vicinity of oil and gas facilities: Lessons learned from a large-scale project. In, *SPE International Conference on Health, Safety, and Environment*: Society of Petroleum Engineers

Dwivedi, R., & Kandrika, S. (2005). Delineation and monitoring of aquaculture areas using multi-temporal space-borne multispectral data. *Current Science*, 1414-1421

Foody, G.M. (2002). Status of land cover classification accuracy assessment. *Remote Sensing of Environment, 80*, 185-201

Friess, D.A., Yando, E.S., Abuchahla, G.M., Adams, J.B., Cannicci, S., Canty, S.W., Cavanaugh, K.C., Connolly, R.M., Cormier, N., Dahdouh-Guebas, F. & Diele, K. (2020). Mangroves give cause for conservation optimism, for now. *Current Biology*, *30*, R153-R154

Gao, J. (1998). A hybrid method toward accurate mapping of mangroves in a marginal habitat from SPOT multispectral data. *International Journal of Remote Sensing, 19*, 1887-1899

Gao, J., Chen, H., Zhang, Y., & Zha, Y. (2004). Knowledge-based approaches to accurate mapping of mangroves from satellite data. *Photogrammetric Engineering & Remote Sensing, 70*, 1241-1248

Giri, C., Long, J., Abbas, S., Murali, R.M., Qamer, F.M., Pengra, B., & Thau, D. (2015). Distribution and dynamics of mangrove forests of South Asia. *Journal of Environmental Management, 148*, 101-111

Giri, C., Ochieng, E., Tieszen, L., Zhu, Z., Singh, A., Loveland, T., Masek, J., & Duke, N. (2011). Status and distribution of mangrove forests of the world using earth observation satellite data. *Global Ecology and Biogeography, 20*, 154-159

Giri, C., Pengra, B., Zhu, Z., Singh, A., & Tieszen, L.L. (2007). Monitoring mangrove forest dynamics of the Sundarbans in Bangladesh and India using multi-temporal satellite data from 1973 to 2000. *Estuarine, Coastal and Shelf Science, 73*, 91-100

Giri, C., Zhu, Z., Tieszen, L., Singh, A., Gillette, S., & Kelmelis, J. (2008). Mangrove forest distributions and dynamics (1975–2005) of the tsunami-affected region of Asia†. *Journal of Biogeography, 35*, 519-528

Goldberg, L., Lagomasino, D., Thomas, N. and Fatoyinbo, T. (2020). Global declines in human-driven mangrove loss. *Global change biology*, *26*, 5844-5855

Green, E., Mumby, P., Edwards, A., Clark, C., & Ellis, A. (1998). The assessment of mangrove areas using high resolution multispectral airborne imagery. *Journal of Coastal Research*, 433-443

Guannel, G., Arkema, K., Ruggiero, P., & Verutes, G. (2016). The power of three: coral reefs, seagrasses and mangroves protect coastal regions and increase their resilience. *PloS one, 11*

Gusmawati, N., Soulard, B., Selmaoui-Folcher, N., Proisy, C., Mustafa, A., Le Gendre, R., Laugier, T., & Lemonnier, H. (2018). Surveying shrimp aquaculture pond activity using multitemporal VHSR satellite images-case study from the Perancak estuary, Bali, Indonesia. *Marine Pollution Bulletin, 131*, 49-60

Hamilton, S. (2013). Assessing the role of commercial aquaculture in displacing mangrove forest. *Bulletin of Marine Science, 89*, 585-601

Hamilton, S.E. (2020). Shrimp Farming. *Mangroves and Aquaculture* (pp. 41-67): Springer

Hamilton, S.E., & Casey, D. (2016). Creation of a high spatio-temporal resolution global database of continuous mangrove forest cover for the 21st century (CGMFC-21). *Global Ecology and Biogeography, 25*, 729-738

Hansen, M.C., Stehman, S.V., Potapov, P.V., Arunarwati, B., Stolle, F., & Pittman, K. (2009). Quantifying changes in the rates of forest clearing in Indonesia from 1990 to 2005 using remotely sensed data sets. *Environmental Research Letters, 4*, 034001

Hariati, A., Wiadnya, D., Prajitno, A., Sukkel, M., Boon, J., & Verdegem, M. (1995). Recent developments of shrimp, Penaeus monodon (Fabricius) and Penaeus merguiensis (de Man), culture in East Java. *Aquaculture Research, 26*, 819-821

Hechanova, R. (1984). Problems on pond construction and maintenance on cat clay soils. *Inland Aquaculture Engineering*

Held, A., Ticehurst, C., Lymburner, L., & Williams, N. (2003). High resolution mapping of tropical mangrove ecosystems using hyperspectral and radar remote sensing. *International Journal of Remote Sensing, 24*, 2739-2759

Heumann, B.W. (2011). An object-based classification of mangroves using a hybrid decision tree—Support vector machine approach. *Remote Sensing, 3*, 2440-2460

Hogarth, P.J. (2015). *The biology of mangroves and seagrasses*. Oxford University Press

Holben, B.N. (1986). Characteristics of maximum-value composite images from temporal AVHRR data. *International Journal of Remote Sensing, 7*, 1417-1434

Ilman, M., Dargusch, P., & Dart, P. (2016). A historical analysis of the drivers of loss and degradation of Indonesia's mangroves. *Land use policy, 54*, 448-459

Irons, J.R., Dwyer, J.L., & Barsi, J.A. (2012). The next Landsat satellite: The Landsat data continuity mission. *Remote Sensing of Environment, 122*, 11-21

Jayanthi, M. (2011). Monitoring brackishwater aquaculture development using multi-spectral satellite data and GIS- a case study near Pichavaram mangroves south-east coast of India. *Indian Journal of Fisheries, 58*, 85-90

Jensen, J.R. (2005). Introductory digital image processing 3rd edition. In: Upper Saddle River: Prentice Hall

Kapetsky, J.M., & Aguilar-Manjarrez, J. (2007). *Geographic information systems, remote sensing and mapping for the development and management of marine aquaculture*. Food & Agriculture Org.

Kathiresan, K., & Bingham, B.L. (2001). Biology of mangroves and mangrove ecosystems. *Advances in marine biology, 40*, 81-251

Kovacs, J., Lu, X., Flores-Verdugo, F., Zhang, C., Flores de Santiago, F., & Jiao, X. (2013). Applications of ALOS PALSAR for monitoring biophysical parameters of a degraded black mangrove (Avicennia germinans) forest. *ISPRS Journal of Photogrammetry and Remote Sensing, 82*, 102-111

Lagomasino, D., Fatoyinbo, T., Lee, S.K., & Simard, M. (2015). High-resolution forest canopy height estimation in an African blue carbon ecosystem. *Remote Sensing in Ecology and Conservation, 1*, 51-60

Lee, S.-K., Fatoyinbo, T.E., Lagomasino, D., Feliciano, E., & Trettin, C. (2018). Multibaseline tandem-x mangrove height estimation: The selection of the vertical wavenumber. *IEEE Journal of Selected Topics in Applied Earth Observations and Remote Sensing*, 1-9

Li, J., & Chen, W. (2005). A rule-based method for mapping Canada's wetlands using optical, radar and DEM data. *International Journal of Remote Sensing, 26*, 5051-5069

Lucas, R., Rebelo, L., Fatoyinbo, L., Rosenqvist, A., Itoh, T., Shimada, M., Simard, M., Souza-Filho, P., Thomas, N., & Trettin, C. (2014). Contribution of L-band SAR to Systematic Global Mangrove Monitoring. *Marine and Freshwater Research*

Lucas, R.M., Mitchell, A.L., Rosenqvist, A., Proisy, C., Melius, A., & Ticehurst, C. (2007). The potential of L-band SAR for quantifying mangrove characteristics and change: case studies from the tropics. *Aquatic Conservation: Marine and Freshwater Ecosystems, 17*, 245-264

McIvor, A., Spencer, T., Moller, I., & Spalding, M. (2012). Storm surge reduction by mangroves. In, *Natural Coastal Protection Series: Report 2* (p. 35 pages)

Meaden, G.J., & Aguilar-Manjarrez, J. (2013). Advances in geographic information systems and remote sensing for fisheries and aquaculture. *FAO Fisheries and Aquaculture Technical Paper*, I

Myint, S.W., Giri, C.P., Wang, L., Zhu, Z., & Gillette, S.C. (2008). Identifying mangrove species and their surrounding land use and land cover classes using an object-oriented approach with a lacunarity spatial measure. *GIScience & Remote Sensing, 45*, 188-208

Nascimento Jr, W.R., Souza-Filho, P.W.M., Proisy, C., Lucas, R.M., & Rosenqvist, A. (2013). Mapping changes in the largest continuous Amazonian mangrove belt using object-based classification of multisensor satellite imagery. *Estuarine, Coastal and Shelf Science*

Pattanaik, C., & Prasad, S.N. (2011). Assessment of aquaculture impact on mangroves of Mahanadi delta (Orissa), East coast of India using remote sensing and GIS. *Ocean & coastal management, 54*, 789-795

Persoon, G.A., & Simarmata, R. (2014). Undoing ‘marginality’: the islands of the Mahakam delta, East Kalimantan (Indonesia). *Journal of Marine and Island Cultures, 3*, 43-53

Prasad, K.A., Ottinger, M., Wei, C., & Leinenkugel, P. (2019). Assessment of Coastal Aquaculture for India from Sentinel-1 SAR Time Series. *Remote Sensing, 11*, 357

Primavera, J.H., Friess, D.A., Van Lavieren, H., & Lee, S.Y. (2019). The Mangrove Ecosystem. *World Seas: an Environmental Evaluation* (pp. 1-34): Elsevier

Proisy, C., Mougin, E., Fromard, F., & Karam, M. (2000). Interpretation of polarimetric radar signatures of mangrove forests. *Remote Sensing of Environment, 71*, 56-66

Rahman, A.F., Dragoni, D., Didan, K., Barreto-Munoz, A., & Hutabarat, J.A. (2013). Detecting large scale conversion of mangroves to aquaculture with change point and mixed-pixel analyses of high-fidelity MODIS data. *Remote Sensing of Environment, 130*, 96-107

Richards, D.R., & Friess, D.A. (2016). Rates and drivers of mangrove deforestation in Southeast Asia, 2000–2012. *Proceedings of the National Academy of Sciences, 113*, 344-349

Rizal, A., Sahidin, A., & Herawati, H. (2018). Economic value estimation of mangrove ecosystems in Indonesia. *Biodiversity International Journal, 2*

Rocha de Souza Pereira, F., Kampel, M., & Cunha-Lignon, M. (2012). Mapping of mangrove forests on the southern coast of São Paulo, Brazil, using synthetic aperture radar data from ALOS/PALSAR. *Remote Sensing Letters, 3*, 567-576

Setiawan, Y., & Pertiwi, D.G.B.C.S. (2014). Evaluation of Land Suitability for Brackishwatershrimp Farming using GIS in Mahakam Delta, Indonesia. *Evaluation, 4*

Shinn, A., Pratoomyot, J., Griffiths, D., Trong, T., Vu, N., Jiravanichpaisal, P., & Briggs, M. (2018). Asian shrimp production and the economic costs of disease. *Asian Fish. Sci. S, 31*, 29-58

Sidik, A.S. (2010). THE CHANGES OF MANGROVE ECOSYSTEM IN MAHAKAM DELTA, INDONESIA: A COMPLEX SOCIALENVIRONMENTAL PATTERN OF LINKAGES IN RESOURCES UTILIZATION. *Borneo Research Journal, 4*, 27-46

Sidik, A.S., Syafril, M., Aristiawan, B., & Bosma, R.W. (2014). Financial Analysis of Tiger Shrimp and Milkfish Pond Farming and Farmer's Motivation in Muara Badak, Mahakam Delta, Indonesia. *Jurnal Ilmu Perikanan Tropis, 19*, 75-84

Simard, M., Zhang, K., Rivera-Monroy, V.H., Ross, M.S., Ruiz, P.L., Castañeda-Moya, E., Twilley, R.R., & Rodriguez, E. (2006). Mapping height and biomass of mangrove forests in Everglades National Park with SRTM elevation data. *Photogrammetric Engineering and Remote Sensing, 72*, 299-311

Sridhar, P., Surendran, A., & Ramana, I. (2008). Auto-extraction technique-based digital classification of saltpans and aquaculture plots using satellite data. *International Journal of Remote Sensing, 29*, 313-323

Stevenson, N. (1997). Disused shrimp ponds: Options for redevelopment of mangroves

Sunarto, A., Koesharyani, I., Supriyadi, H., Gardenia, L., Sugianti, B., & Rukmono, D. (2004). Current status of transboundary fish diseases in Indonesia: Occurrence, surveillance, research and training. In, *Transboundary Fish Diseases in Southeast Asia: Occurence, Surveillance, Research and Training. Proceedings of the Meeting on Current Status of Transboundary Fish Diseases in Southeast Asia: Occurence, Surveillance, Research and Training, Manila, Philippines, 23-24 June 2004* (pp. 91-121): Aquaculture Department, Southeast Asian Fisheries Development Center

Travaglia, C., Kapetsky, J.M., Profeti, G., Travaglia, C., Kapetsky, J., & Profeti, G. (1999). *Inventory and monitoring of shrimp farms in Sri Lanka by ERS SAR data*. Food and Agriculture Organization of the United Nations

Travaglia, C., Profeti, G., Aguilar-Manjarrez, J., & Lopez, N.A. (2004). *Mapping coastal aquaculture and fisheries structures by satellite imaging radar: case study of the Lingayen Gulf, the Philippines*. Food & Agriculture Org.

Trisasongko, B.H. (2009). Tropical mangrove mapping using fully-polarimetric radar data. *Journal of Mathematical and Fundamental Sciences, 41*, 98-109

Van Zwieten, P., Sidik, S., Noryadi, I., & Suyatna, I. (2006). Aquatic food production in the coastal zone: data-based perceptions on the trade-off between mariculture and fisheries production of the Mahakam delta and estuary, East Kalimantan, Indonesia.

Environment and Livelihoods in Tropical Coastal Zones: Managing agriculture-fishery-aquaculture-conflicts (pp. 219-236)

Venkataratnam, L., Thammappa, S., Sankar, T.R., & Anis, S. (1997). Mapping and monitoring prawn farming areas through remote sensing techniques. *Geocarto International, 12*, 23-29

Virdis, S.G.P. (2013). An object-based image analysis approach for aquaculture ponds precise mapping and monitoring: a case study of Tam Giang-Cau Hai Lagoon, Vietnam. *Environmental monitoring and assessment*, 1-17

Vo, Q.T., Oppelt, N., Leinenkugel, P., & Kuenzer, C. (2013). Remote sensing in mapping mangrove ecosystems—An object-based approach. *Remote Sensing, 5*, 183-201

Wang, Y., & Imhoff, M. (1993). Simulated and observed L-HH radar backscatter from tropical mangrove forests. *International Journal of Remote Sensing, 14*, 2819-2828

XU, J., ZHAO, J., ZHANG, F., & LI, F. (2013). Object-oriented information extraction of pond aquaculture [J]. *Remote Sensing for Land & Resources, 1*

Zhang, T., Li, Q., Yang, X., Zhou, C., & Su, F. (2010). Automatic mapping aquaculture in coastal zone from TM imagery with OBIA approach. In, *2010 18th International Conference on Geoinformatics* (pp. 1-4): IEEE

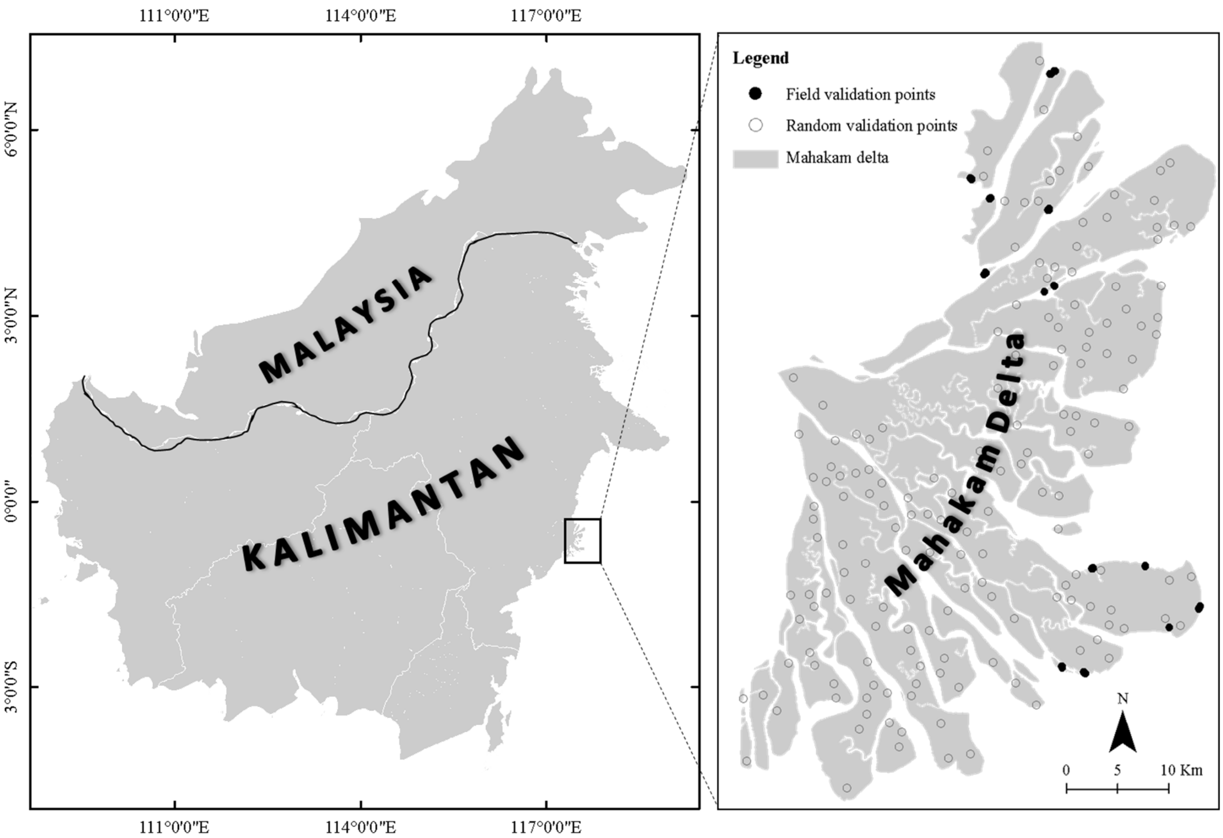

Figure 1. Map of the study area (the Mahakam Delta) in East Kalimantan province of Indonesia. Locations of field-based validation points and Google Earth based random validation points are shown on the delta in the close-up on the right-hand side.

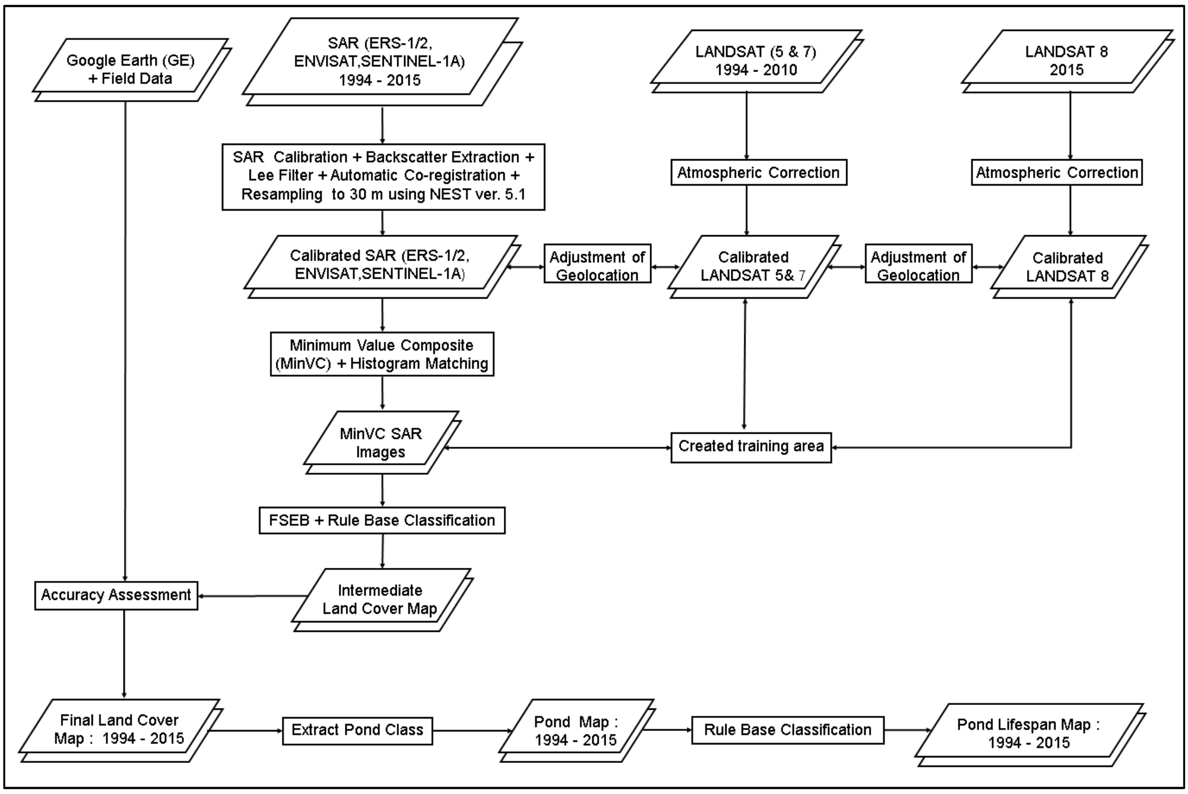

Figure 2. Flowchart of the data processing steps used in this study.

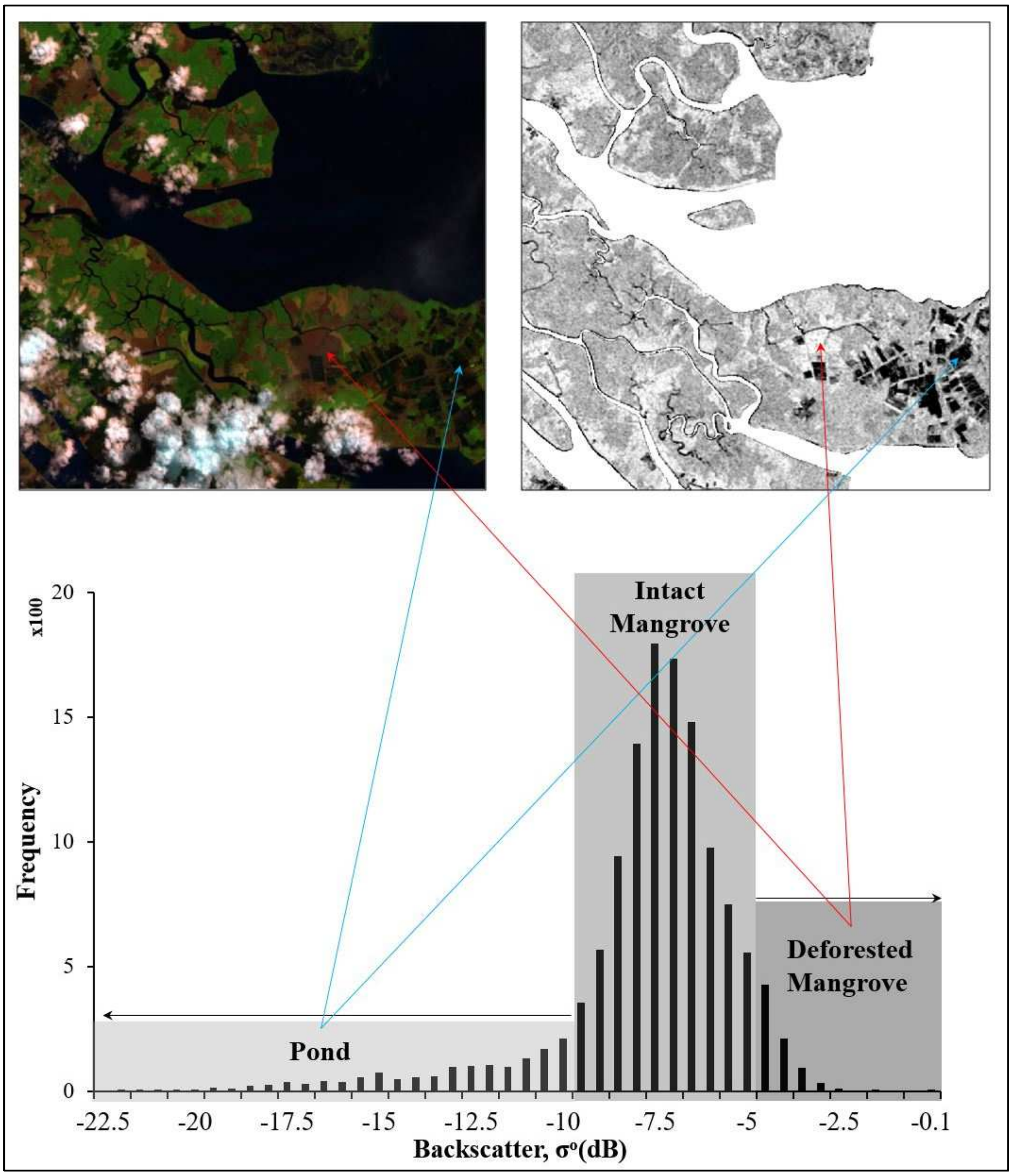

Figure 3. An example of a MinVC processed SAR image of 1997 (top right), false color composite Landsat-5 of 1997 (top left, R=SWIR, G=NIR, and B=Red bands) and corresponding histogram of the backscatter values (bottom). Radar backscatter ranges differ from Landsat pseudo color combinations for aquaculture ponds (black vs. dark blue), deforested mangroves (very bright vs. brown), and primary mangroves (moderate bright vs. green).

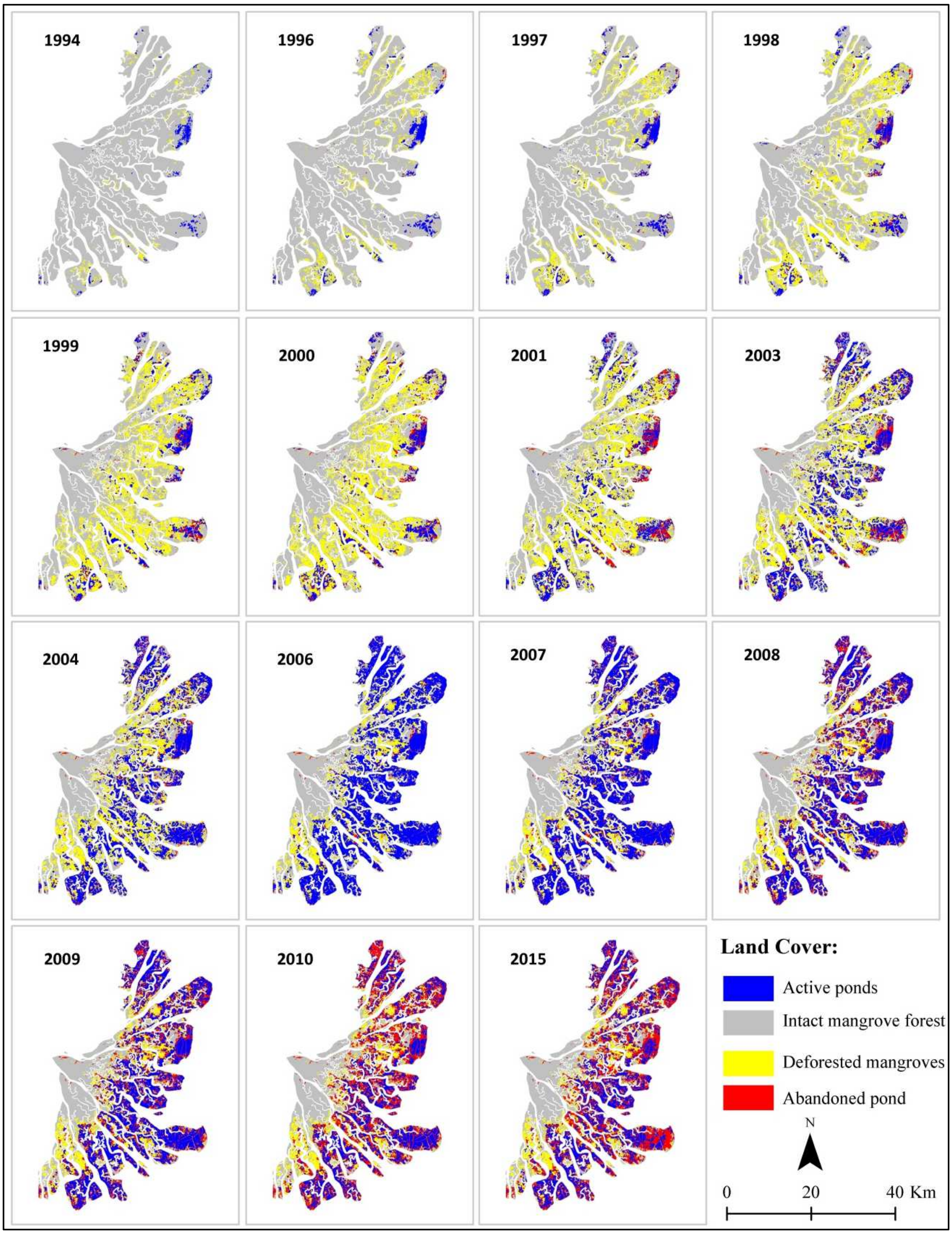

Figure 4. Land cover maps of 15 individual years representing the 1994-2015 period, showing different stages of conversion of mangroves to shrimp and fish ponds, and the subsequent abandonment of ponds in the Mahakam Delta.

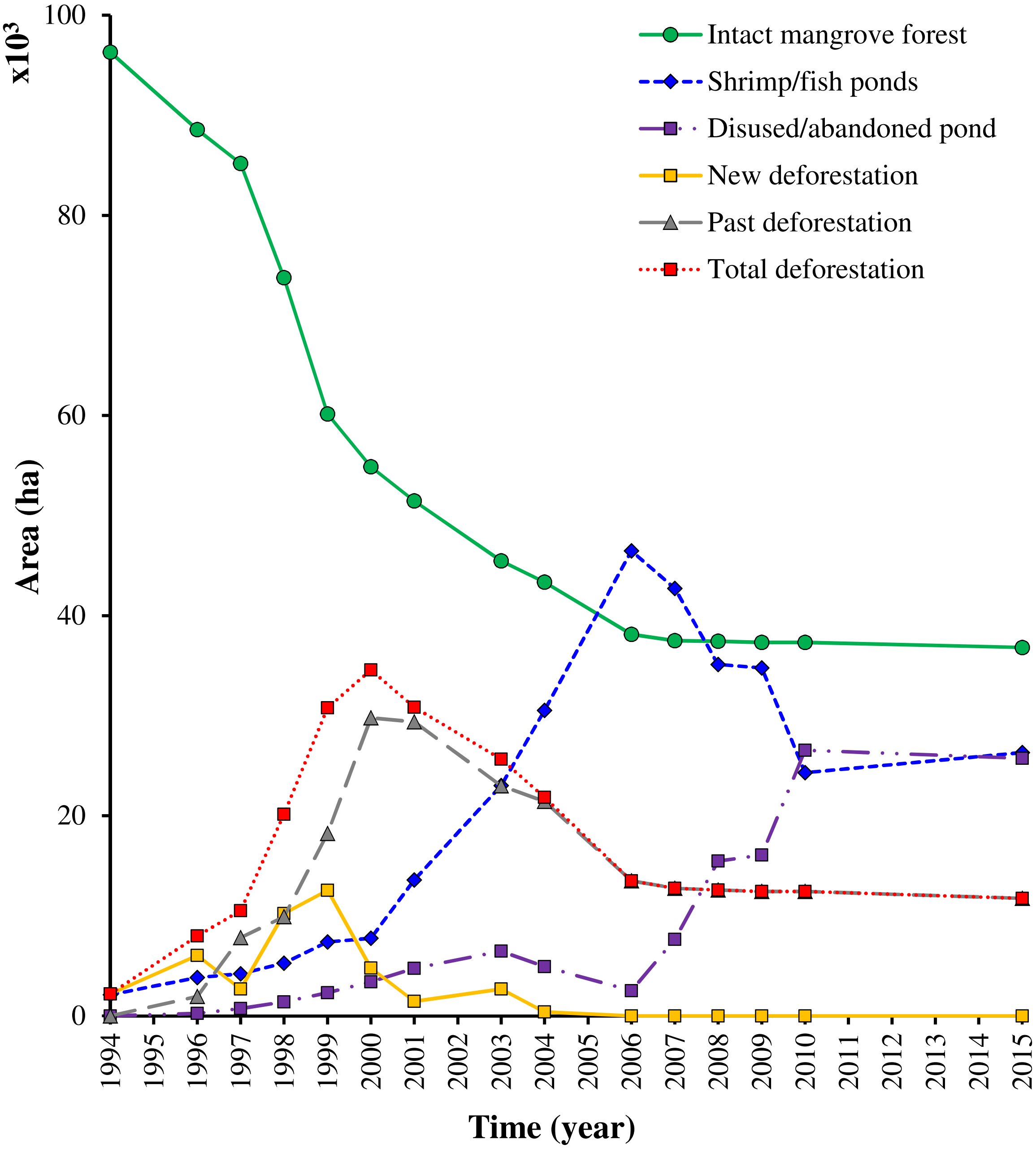

Figure 5. Graphs showing trajectories of 22 years of land cover changes due to anthropogenic disturbance in the Mahakam Delta.

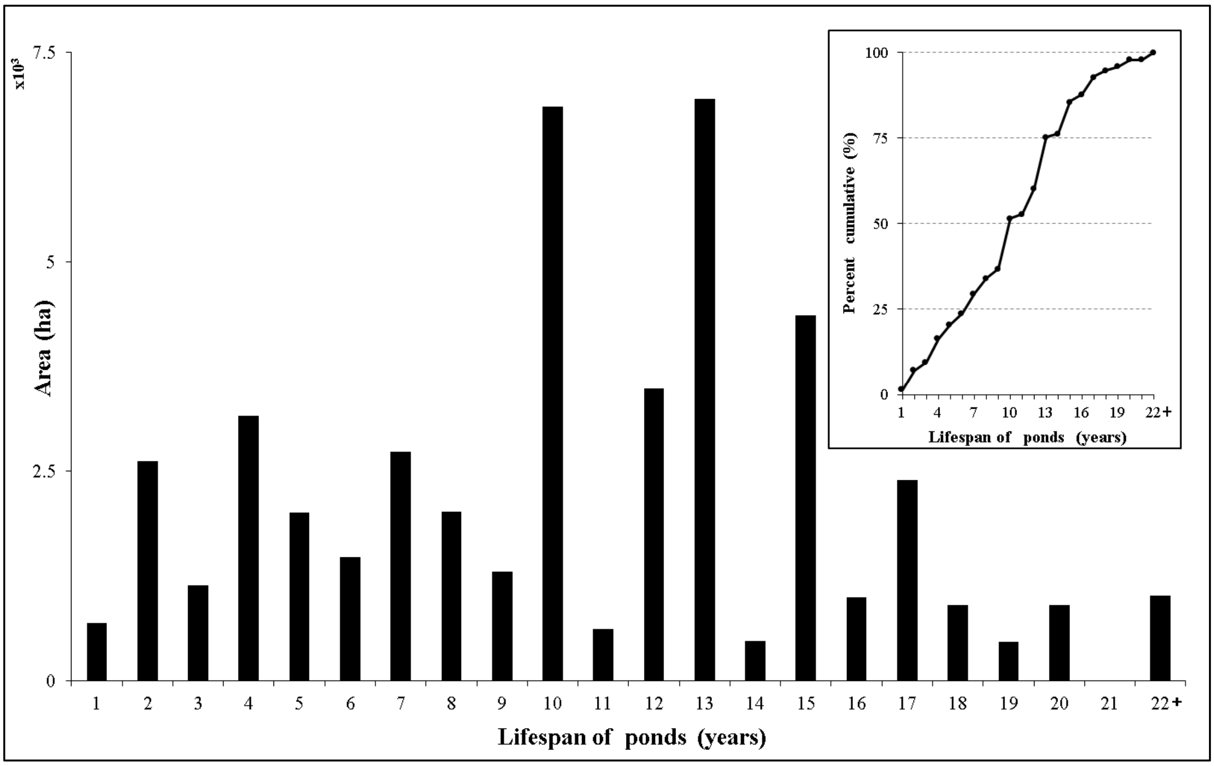

Figure 6. Lifespan of ponds in the Mahakam Delta are shown as area vs. years, with the cumulative distribution shown in the inset.

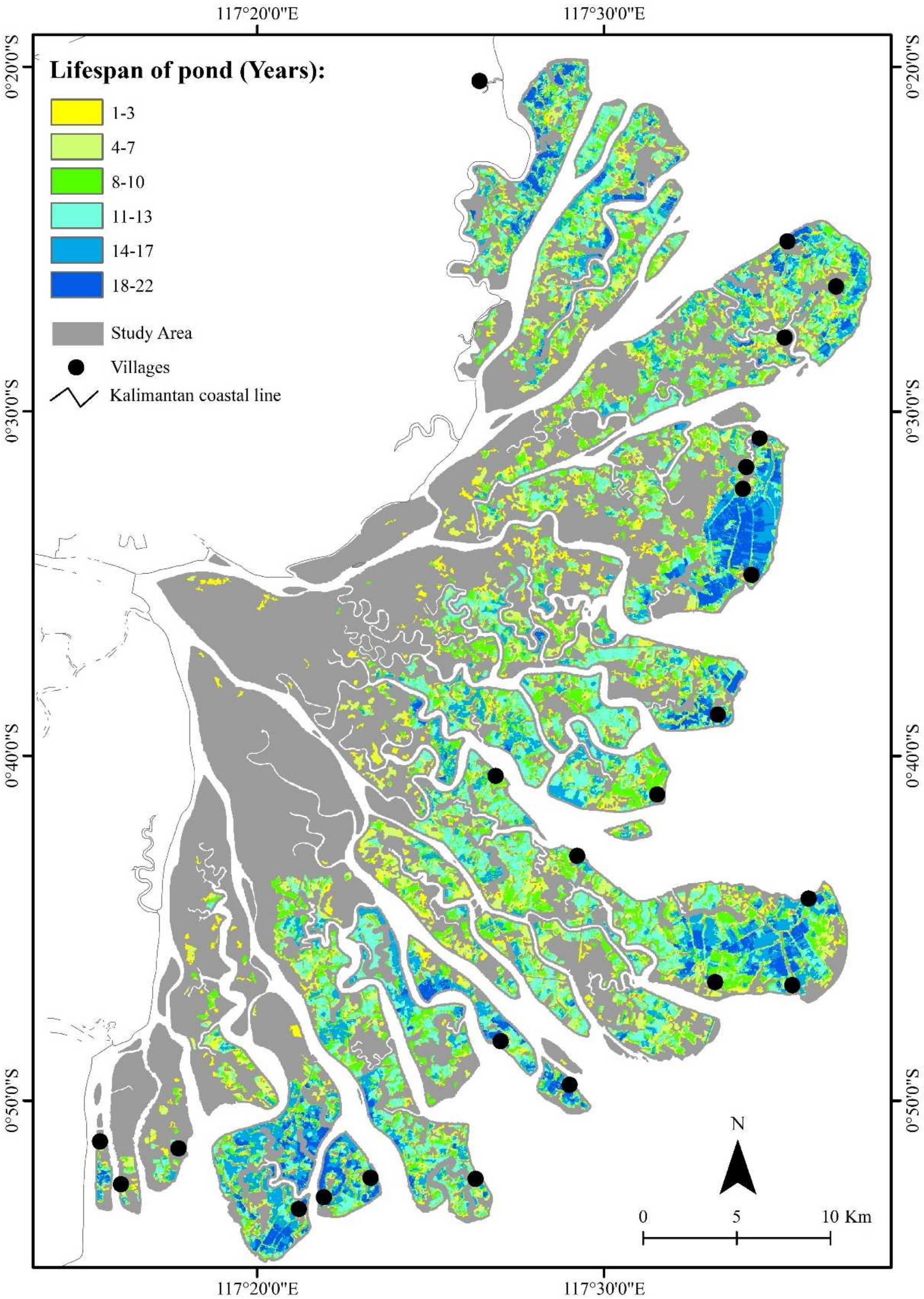

Figure 7. Lifespan map of ponds in the Mahakam Delta shows ponds with longer lifespans were located near the villages. Locations of villages are adopted from (Persoon and Simarmata 2014).

Table 1. List of the SAR datasets used in this study.

No	Date Acquired	Sensor	Mode	Track	No	Date Acquired	Sensor	Mode	Track
1	8-Oct-94	ERS-1	IMP	89	33	18-Apr-01	ERS-2	IMS	418
2	20-Nov-94	ERS-1	IMP	713	34	5-Sep-01	ERS-2	IMS	418
3	3-Jul-96	ERS-2	IMP	418	35	19-Nov-03	ENVISAT	IMS	418
4	7-Aug-96	ERS-2	IMP	418	36	24-Dec-03	ENVISAT	IMS	418
5	23-Apr-96	ERS-1	IMP	418	37	4-Apr-04	ENVISAT	IMP	418
6	24-Apr-96	ERS-2	IMS	418	38	12-May-04	ENVISAT	IMP	418
7	28-May-96	ERS-1	IMS	418	39	16-Jun-04	ENVISAT	IMP	418
8	29-May-96	ERS-2	IMS	418	40	26-Jul-06	ENVISAT	IMP	418
9	3-Jul-96	ERS-2	IMS	418	41	5-Aug-06	ENVISAT	IMP	67
10	7-Aug-96	ERS-2	IMS	418	42	27-Aug-06	ENVISAT	IMP	375
11	11-Sep-96	ERS-2	IMS	418	43	14-Oct-06	ENVISAT	IMP	67
12	16-Oct-96	ERS-2	IMS	418	44	18-Nov-06	ENVISAT	IMP	67
13	25-Dec-96	ERS-2	IMS	418	45	10-Dec-06	ENVISAT	IMP	375
14	14-May-97	ERS-2	IMP	418	46	18-Feb-07	ENVISAT	IMP	375
15	29-Jan-97	ERS-2	IMS	418	47	8-Jul-07	ENVISAT	IMP	375
16	9-Apr-97	ERS-2	IMS	418	48	12-Aug-07	ENVISAT	IMP	375
17	18-Jun-97	ERS-2	IMS	418	49	16-Sep-07	ENVISAT	IMP	375
18	23-Jul-97	ERS-2	IMS	418	50	9-Mar-08	ENVISAT	IMP	375
19	27-Aug-97	ERS-2	IMS	418	51	13-Apr-08	ENVISAT	IMP	375
20	30-Sep-97	ERS-1	IMS	418	52	5-Oct-08	ENVISAT	IMP	375
21	1-Oct-97	ERS-2	IMS	418	53	14-Dec-08	ENVISAT	IMP	375
22	5-Nov-97	ERS-2	IMS	418	54	2-Jan-09	ENVISAT	IMP	146
23	10-Dec-97	ERS-2	IMS	418	55	15-Jan-09	ENVISAT	IMP	339
24	8-Jul-98	ERS-2	IMP	418	56	18-Jan-09	ENVISAT	IMP	375
25	14-Jan-98	ERS-2	IMS	418	57	3-May-09	ENVISAT	IMP	375
26	18-Feb-98	ERS-2	IMS	418	58	16-Aug-09	ENVISAT	IMP	375
27	3-Jun-98	ERS-2	IMS	418	59	14-Mar-10	ENVISAT	IMP	375
28	8-Jul-98	ERS-2	IMS	418	60	18-Apr-10	ENVISAT	IMP	375
29	15-Dec-99	ERS-2	IMP	418	61	23-May-10	ENVISAT	IMP	375
30	19-Jan-00	ERS-2	IMS	418	62	19-Nov-15	SENTINEL-1A	GRD	32
31	22-Feb-00	ERS-1	IMS	418	63	13-Dec-15	SENTINEL-1A	GRD	32
32	23-Feb-00	ERS-2	IMS	418					

Table 2. Backscatter threshold values used for identifying ponds and deforested mangrove areas and their corresponding number of MinVC SAR training pixels used in the FSEB method.

Year	Aquaculture Pond		Deforested Mangrove	
	Threshold value (dB)	**# Pixels for training area**	**Threshold value (dB)**	**# Pixels for training area**
1994	-10.6	1520	-5.47	819
1996	-11.96	1627	-6.29	895
1997	-11.07	1326	-5.93	819
1998	-9.38	1123	-4.81	1729
1999	-9.74	1334	-5.07	2986
2000	-9.96	710	-6	2381
2001	-9.38	511	-5.62	630
2003	-10.95	812	-6.49	1005
2004	-12	611	**	**
2006	-12.08	366	**	**
2007	-10.05	1159	**	**
2008	-12.07	736	**	**
2009	-12.27	670	**	**
2010	-11.19	422	**	**
2015	-12.24	1954	**	**

** No 'new deforestation' was detected since 2004.

Table 3. Accuracy matrix of 2015 land cover map showed producer's, user's, and kappa statistics for each class cover types.

Class Name	Area (ha)	Reference	Classified	# Correct	Producer's (%)	User's (%)	Kappa
Aquaculture pond	26,319	83	71	68	81.93	95.77	0.95
Mangrove forest	36,817	210	205	193	91.9	94.15	0.87
Deforested mangrove	11,749	24	30	23	95.83	76.67	0.75
Abandoned pond	25,744	56	67	47	83.93	70.15	0.65
Totals	100,629	373	373	331			
Overall accuracy: 88.74%; Overall Kappa statistic: 0.82							

Table 4. Total areas of aquaculture ponds developed and abandoned in different years of this study.

Year	Aquaculture Pond (ha/yr)	Abandoned pond (ha/yr)
1994	-	-
1995	994*	-
1996	994*	8
1997	650	3
1998	180	36
1999	3351	43
2000	2062	21
2001	8130	70
2002	6433*	118*
2003	6433*	118*
2004	8109	96
2005	7729*	165*
2006	7729*	165*
2007	374	1139
2008	597	3574
2009	829	749
2010	312	3726
2011	1277*	834*
2012	1277*	834*
2013	1277*	834*
2014	1277*	834*
2015	1277*	834*

* Average values due to unavailability of SAR data (see Fig. 6). For example, in 2015, a total of ~6,382 ha was classified as new aquaculture ponds. Since no data were available for 2011-2014, we distributed the 6382 ha over 5 years (2011-2015), therefore allocating 1277 ha for each of these years. Similar procedure was applied for abandoned ponds.

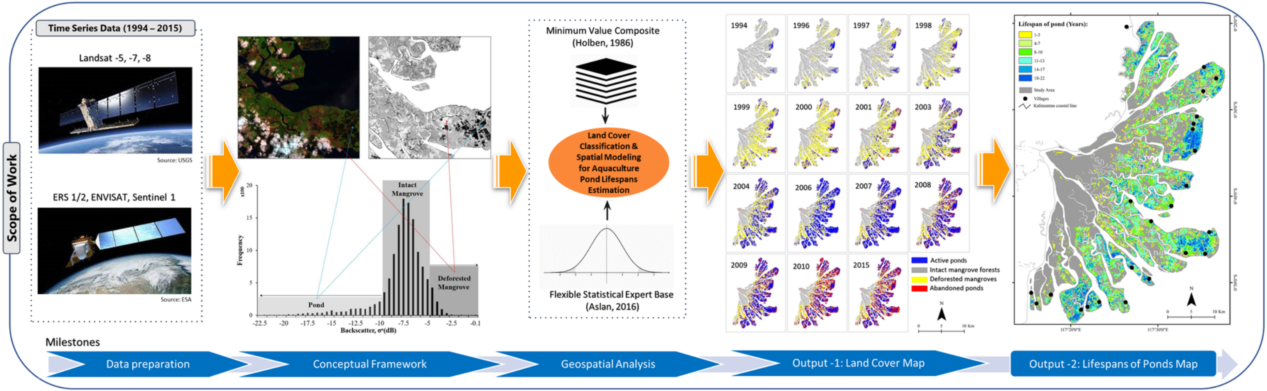
Scope of Work
Time Series Data (1994 – 2015)
Landsat -5, -7, -8
Source: USGS
ERS 1/2, ENVISAT, Sentinel 1
Source: ESA
Intact Mangrove
Deforested Mangrove
Pond
Frequency
x100
Backscatter, σ°(dB)
Minimum Value Composite (Holben, 1986)
Land Cover Classification & Spatial Modeling for Aquaculture Pond Lifespans Estimation
Flexible Statistical Expert Base (Aslan, 2016)
1994
1996
1997
1998
1999
2000
2001
2003
2004
2006
2007
2008
2009
2010
2015
Active ponds
Intact mangrove forests
Deforested mangroves
Abandoned ponds
Lifespan of pond (Years):
1-3
4-7
8-10
11-13
14-17
18-22
Study Area
Villages
Kalimantan coastal line
Milestones
Data preparation
Conceptual Framework
Geospatial Analysis
Output -1: Land Cover Map
Output -2: Lifespans of Ponds Map